Composition and Crystallization of Milk Fat Fractions

G.A. van Aken[a,*], E. ten Grotenhuis[a], A.J. van Langevelde[b], and H. Schenk[b]

[a]Netherlands Institute for Dairy Research (NIZO), Department of Technology, 6710 BA Ede, The Netherlands and [b]Institute for Molecular Chemistry (IMC), Laboratory of Crystallography, Universiteit van Amsterdam, 1018 WV Amsterdam, The Netherlands

ABSTRACT: Milk fat was fractionated by solvent (acetone) fractionation and dry fractionation. Based on their fatty acid and acyl-carbon profiles, the fractions could be divided into three main groups: high-melting triglycerides (HMT), middle-melting triglycerides (MMT), and low-melting triglycerides (LMT). HMT fractions were enriched in long-chain fatty acids, and reduced in short-chain fatty acids and unsaturated fatty acids. The MMT fractions were enriched in long-chain fatty acids, and reduced in unsaturated fatty acids. The LMT fractions were reduced in long-chain fatty acids, and enriched in short-chain fatty acids and unsaturated fatty acids. Crystallization of these fractions was studied by differential scanning calorimetry and X-ray diffraction techniques. In this study, the stable crystal form appeared to be the β′-form for all fractions. At sufficiently low temperature (different for each fraction), the β′-form is preceded by crystallization in the metastable α-form. An important difference between the fractions is the rate of crystallization in the β′-form, which proceeds at a much lower rate for the lower-melting fat fractions than for the higher-melting fat fractions. This may be due to the much lower affinity for crystallization of the lower-melting fractions, due to the less favorable molecular geometry for packing in the β′-crystal lattice.

Paper no. J9080 in *JAOCS 76*, 1323–1331 (November 1999).

KEY WORDS: Crystallization, differential scanning calorimetry, fractionation, milk fat, polymorphism, triglyceride, X-ray diffraction.

Milk fat is a natural product obtained from cream, and it forms the main constituent of butter. It has excellent organoleptic properties, which makes it an important ingredient in the bakery and confectionery industry. Despite these good qualifications, the market for milk fat has tended to decline in recent years due to its high price and limited functional properties. Melting characteristics and firmness vary with the season, breed of cow, stage of lactation, and the feed given to the cows. Moreover, the product diversity of milk fat is limited compared to that of margarine, for which a whole range of products exists for applications such as puff pastry, cookies, and cold-spreadable products.

*To whom correspondence should be addressed at NIZO food research, Dept. of Technology, P.O. Box 20, 6710 BA Ede, The Netherlands. E-mail: aken@nizo.nl

The physical properties of milk fat are determined by triglycerides, which are its main components. These triglycerides are composed of a large number of different fatty acids. This leads to a heterogeneous composition of triglycerides and a very broad melting range, which varies between approximately –40 and 35°C. Characteristic for milk fat is the occurrence of large amounts (approximately 25% on a molar basis) of short-chain fatty acids, of which butyric acid is the most important.

Polymorphism is a common property of all triglycerides (1,2), including milk fat. The main types of polymorphic crystal forms in triglycerides are the γ-, α-, β′-, and β-forms (3–5). Of these main types, either the β′- or β-form is the stable form, depending on the molecular geometry of the triglyceride (6). The other forms are metastable, although they may persist for a long time. For milk fat, the β′-form is the most stable.

The utilization range of milk fat can be broadened by separating it into fractions with different melting ranges (7,8). Much literature has been devoted to this subject, and a good overview has been presented by Kaylegian and Lindsay (9). The most important fractionation process is dry fractionation (9–14). Other processes, such as detergent fractionation and solvent fractionation (including supercritical CO_2-fractionation), are not applied to milk fat on a commercial scale due to the high costs, use of solvents, or flavor deterioration (15).

In the literature, milk fat is usually separated into three main fractions with very different melting points: low-melting fat (LMF), middle-melting fat (MMF), and high-melting fat (HMF) (16). It is often assumed that these main fractions would crystallize separately, and thus would behave as more or less independent pseudocomponents (*cf.* 16,17). This view was supported by the occurrence of three main endothermic peaks in a heating thermogram recorded by differential scanning calorimetry (DSC) (13,16,18). However, the crystallization and melting of milk fat are complicated by the occurrence of transitions between several polymorphic crystal forms, and ten Grotenhuis *et al.* (3) recently showed that the particular shape of the curve with three main peaks is only observed when the DSC curve is recorded in a specific way. X-ray powder diffraction revealed that the shape of the curve is partly due to a polymorphic transformation during heating.

The main purpose of this work was to investigate whether the separation of milk fat into a number of main fractions is fun-

damentally due to its composition or if this separation is merely due to arbitrary choices in the fractionation temperatures. To investigate this, milk fat was fractionated by acetone and dry fractionation. The resulting fractions were analyzed chemically (fatty acid distribution and acyl-carbon number profile) and physically (X-ray powder diffraction and DSC) to see if a grouping of triglycerides can be achieved based on their mutual miscibility in the solid state or their solubility in acetone.

MATERIALS AND METHODS

Milk fat. Anhydrous milk fat, produced in the winter season of 1996, was obtained from Frico Union de Jong (Noordwijk (Gr.), The Netherlands).

Acetone fractionation. Milk fat (50 g) was dissolved in acetone in a concentration of 13.3 g milk fat per 100 mL acetone at a temperature of 45°C. The temperature was lowered to 40°C and the solution was left to crystallize for 24 h. The fat crystals were separated by vacuum filtration and the filtrate was kept for further fractionation. Fractionation was repeated at crystallization temperatures of 40, 25, 20, 15, 10, 5, 2, 0, –5, –13, –20, and –25°C. Each time, the volume of the filtrate was adjusted to 100 mL with acetone, after which the solution was heated to 45°C, cooled to the desired crystallization temperature, and left to crystallize for 24 h before filtration. The retentates and the filtrate of –25°C were dried at 65°C to remove the acetone.

Dry fractionation. Crystallization was carried out in a thermostatted, stirred crystallization tank built by Terlet (Zutphen, the Netherlands). Nine hundred kilograms of milk fat was heated to 65°C to destroy all crystal nuclei, slowly cooled to 24°C, and stored at this temperature for 24 h. During the storage time, the crystallizing mass was periodically stirred (every 15 min for a period of 3 min at a stirring speed of 10 rpm). To minimize oxidation, the head space of the tank was filled with nitrogen. The solid and liquid fractions were separated at 24°C on a rotary belt vacuum filter built by Nivoba (Veendam, The Netherlands). Part of the solid fraction (S24) was fractionated by melting at 65°C and stored for 24 h at 30°C. Filtration at 30°C led to a solid mass (S30) and a liquid (L30). Similarly, the filtrate (L24) obtained at 24°C was fractionated at 19°C, leading to the fractions S19 and L19. Finally, the liquid fraction L19 was fractionated at 11°C, yielding the fractions S11 and L11. The multistage dry fractionation procedure is outlined in Scheme 1.

Fatty acid analysis. Glass capillary gas chromatography of fatty acid methyl esters derived from the fat samples was used to determine the fatty acid profile. The method is described in detail by Badings and de Jong (19). Usually, 35 different fatty acids could be detected. For clarity, however, only the main fatty acids and groups of fatty acids (e.g., $C_{18:1}$ as the sum for all positions of the double bond) are reported.

Acyl-carbon number profiles. Automated triglyceride analyses were carried out on a CE Mega 5360 gas chromatograph equipped with a flame-ionization detector, a high oven temperature cold-on-column (H.O.T.) injector and a model

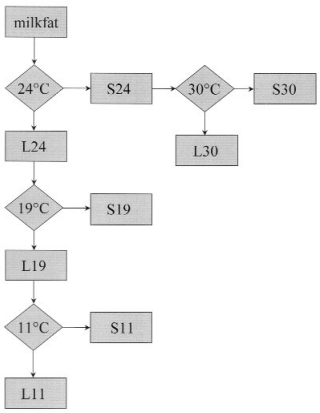

SCHEME 1

AS-550 CE autosampler (setup by CE Instruments, Thermo Quest, Milano, Italy). The instrument was fitted with a 10 m × 0.32 mm CP Sil 5CB HT (d_f = 0.1 m) fused-silica column (Varian-Gronpack, Middelburg, The Netherlands). Hydrogen carrier gas was used with an inlet pressure of 30 kPa. Samples (0.02% fat in heptane) were injected into the column at an oven temperature of 200°C with secondary cooling of the injection zone. The temperature program of the oven was started 1 min after injection to raise the temperature to 300°C at 10°C/min, and then to 350°C at 4°C/min. The results were expressed as peak area percentages. For the analytical procedure used, the peak area percentages correspond to weight fraction percentages of triglycerides. The validity of this equality was checked for each series of samples using a milk fat sample of accurately known composition.

DSC. The heat exchange of milk fat with the environment during cooling, heating, and isothermal storage was measured with a differential scanning calorimeter (Perkin Elmer DSC 7; Perkin Elmer Nederland, Nieuwerkerk aan de IJssel). Samples of 10 mg were weighed in aluminum measuring pans, which were sealed and placed into the calorimeter. An empty sealed pan was used for reference.

DSC heating curves were determined by holding the samples for 1 min at 70°C to completely melt the fat and eliminate all crystal nuclei, after which the samples were cooled to –65°C at a cooling rate of 5°C/min. The samples were kept for 1 min at –65°C before heating to 70°C at a preset heating rate. The clear points were obtained from DSC heating curves as the temperature above which no heat flow related to melting could be measured.

Isothermal DSC curves were determined by holding the samples for 1 min at 70°C to completely melt the fat and eliminate all crystal nuclei, after which the samples were cooled at 5°C/min to the measuring temperature. The samples were kept at this temperature while recording the isothermal heat effect. At the end of the isothermal period, the samples were heated to 70°C at 5°C/min while measuring the melting behavior.

X-ray diffraction (XRD). XRD patterns were recorded with an instrument by Van Malssen *et al.* (20). Samples were first heated to 70°C and held at this temperature for 5 min to elim-

inate all nuclei. Next, the samples were cooled at 20°C/min to the temperature of crystallization, after which the development of the XRD pattern was recorded. Monochromated copper K_α radiation with a wavelength of 1.5418 Å was used to obtain diffraction patterns in the 2θ range of 14.6–29.6°, which correspond to lattice-spacing from 3.0 to 6.1 Å; this range contains the diffraction patterns characteristic for the different triglyceride crystal polymorphs. The instrument was calibrated with potassium iodide as a reference. The samples were prepared by pressing solid samples into a sample holder with dimensions of $1 \times 10 \times 15$ mm^3. The sample holder supported a mass of fat sample of approximately 135 mg. The sample holder was positioned in a vacuum measuring chamber. The temperature of the sample holder was controlled by simultaneous cooling with water or liquid nitrogen and heating using a TTK-HC temperature controller (Anton PAAR KG, Graz, Austria). Accuracy in measured temperature = 0.1°C. All XRD patterns are represented as difference patterns with respect to liquid milk fat.

RESULTS

Acetone fractionation. Table 1 lists the amounts of fat separated at each fractionation temperature. A cumulative plot of these data is given in Figure 1. A relatively smooth curve is obtained, showing only one slight "hill" around 0°C. The smoothness of the curve indicates that no sharp separation between the different triglycerides was obtained; only a gradual separation into fractions was achieved.

Figure 2 shows the DSC heating curves for acetone fractions separated at the various temperatures. The clear points of the acetone fractions are given in Table 1. The curves are similar to those found by Lohman and Hartel (21) for acetone fractions obtained at temperatures between 25 and 0°C. The DSC curve of the fraction separated at 25°C deviates from the general trend in the series of DSC curves. This is probably due to the inclusion of a large amount of milk fat in the separated crystal mass, and must therefore be considered an artifact. The sequence of curves in Figure 2 reflects a division into three main groups of triglycerides, HMT, MMT, and LMT (high-, middle-, and low-melting triglycerides, respectively) in descending order of clear point. It would appear that these fractions do not fully correspond to HMF, MMF, and LMF as defined by Timms (16). HMT consists of the fractions separated at temperatures between 25 and 10°C. According to Table 1, approximately 31% of the triglycerides belong to this group. MMT is separated at temperatures between 5 and −5°C, and forms approximately 34% of the triglycerides. The slight "hill" in the curve of Figure 2 is probably due to the crystallization of MMT. At temperatures of −13°C and below, LMT is separated, which forms approximately 36% of the triglycerides.

The DSC curves of both the LMT and the HMT group of fractions show only one endothermic peak, whereas the DSC curves of the MMT group of fractions show two or more endothermic peaks. In the DSC heating curves of the HMT group of fractions, the endothermic peak is preceded by an exothermic heat effect in the DSC heating curve. This effect was also observed by Lohman and Hartel (21). XRD indicated that this exothermic effect is due to the formation of β′-crystals (data not shown), similar to the transition observed in milk fat described by ten Grotenhuis *et al.* (3). The LMT group of fractions does not show such an exothermic heat effect, resulting in only a single endothermic melting peak in the DSC heating curve. The reason for this difference will be explained in the dry fractionation section.

Tables 2 and 3 give the fatty acid and acyl-carbon number profiles for the acetone fractions. From these tables, the following general trends can be deduced. Table 2 shows that HMT fractions obtained by acetone fractionation are enriched in $C_{16:0}$ and $C_{18:0}$, and reduced in the short-chain fatty acid (e.g., $C_{4:0}$) and unsaturated fatty acid (e.g., $C_{18:1}$) contents. The MMT fractions are enriched in $C_{16:0}$ and $C_{18:0}$ and reduced in the unsaturated fatty acid (e.g., $C_{18:1}$) contents. The

TABLE 1
Relative Amounts and Clear Points of the Fractions Obtained by Acetone Fractionation

Fraction[a]	Relative amount (weight %)	Clear point (°C)
Milk fat	100	35
S25	9.66	44
S20	7.16	50
S15	6.21	43
S10	7.38	44
S5	7.13	34
S2	5.80	—
S0	13.10	25
S–5	7.51	21
S–13	3.12	15
S–20	9.63	10
S–25	3.63	5
L–25	19.66	–9

[a]S, solid fraction; L, liquid fraction. Numbers following the type of fraction (S or L) correspond to the temperature at which the fraction separated (25 to –25°C).

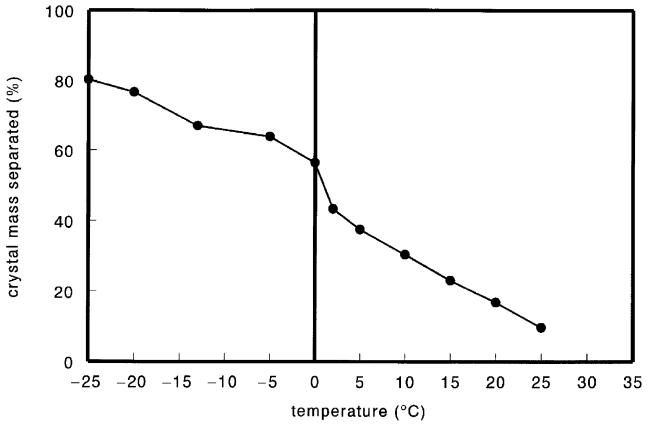

FIG. 1. Cumulative plot of the crystal mass separated by acetone fractionation as a function of temperature.

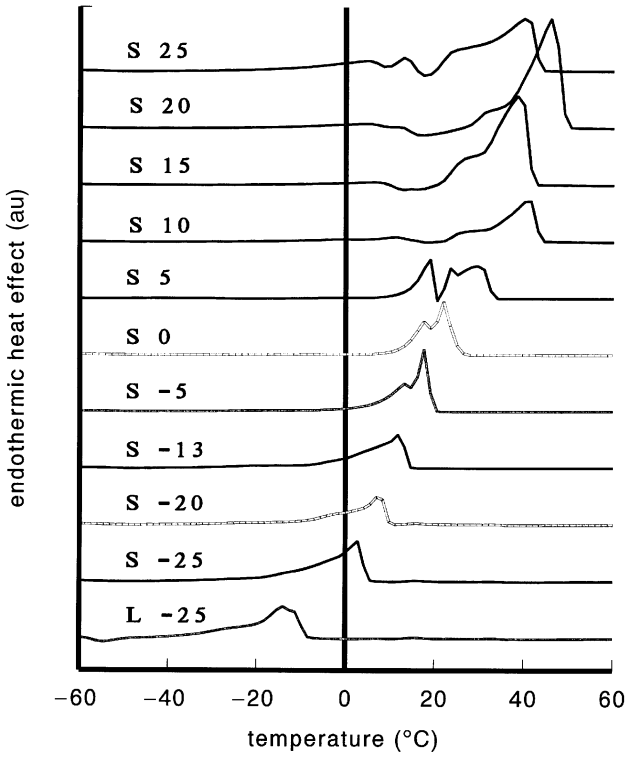

FIG. 2. Differential scanning calorimetry (DSC) heating curves of the acetone fractions.

LMT fractions obtained by acetone fractionation are reduced in $C_{16:0}$ and $C_{18:0}$ and enriched in short-chain fatty acids and unsaturated fatty acids. Table 3 shows that for the HMT fractions, the content of TG26–40 appears to be reduced whereas the content of TG44–54 appears to be increased. The MMT fraction is reduced in TG26–34, and the contents of TG42–44 and TG50 vary from increased to reduced for fractions separated between 5 and −5°C. The LMT fractions are increased in TG26–36 and reduced in TG44–52.

Dry fractionation. Table 4 gives the relative quantities and the clear points of the different fractions obtained by dry fractionation. The DSC curves of the fractions separated by crystallization are given in Figure 3. S24 and S30 are the HMT fractions. The DSC curves of the HMT fractions (S24 and S30) are different from the curves obtained by acetone fractionation, and are characterized by a broad shoulder between 20 and 40°C. S24 forms 63% of the total amount of milk fat (S30 was obtained from S24 by a second fractionation). S19 and S11 are the MMT fractions, which form approximately 29% of the total amount of fat. The DSC curve of S11 resembles the curve obtained for acetone fractions S0 and S–5. L11 is the LMT fraction, corresponding to 7% of the total amount of milk fat. Its DSC curve resembles that of acetone fraction S–20.

The fatty acid distributions of the main fatty acids and total chain length distributions of the main triglycerides are compared to the values of the original milk fat in Tables 5 and 6, respectively. The changes with respect to milk fat observed for LMT, MMT, and HMT fractions obtained by dry fractionation are similar to those observed for acetone fractionation, but the effects are generally much smaller. This difference is usually ascribed to the inclusion of rather large amounts of liquid fat in the crystalline fraction separated with dry fractionation, whereas with acetone fractionation, only a dilute solution of the remaining triglycerides is incorporated in the crystalline fraction (9). This leads to a relatively large amount of HMT fractions with lower purity and smaller amounts of the LMT fractions, which is in accordance with our results (Table 4). Another reason for the differences between acetone fractionation and dry fractionation might be that dry fractionation is based on the solubility of the triglycerides in a liquid triglyceride, whereas acetone fraction is based on the solubility in acetone.

Isothermal crystallization of fractions obtained by dry fractionation. Isothermal crystallization was studied for the fractions obtained by dry fractionation. Figure 4 shows a typical series of DSC curves obtained by isothermal crystallization recorded for a range of temperatures between 16 and 26°C for fraction S30. Two exothermic peaks in the DSC curves were observed in the temperature range of 18 to 23°C. At higher temperatures, only one peak was observed. The position of the maximum of this peak shifted to longer times for higher temperatures. XRD measurements were carried out to investigate the transitions taking place during the two exothermic peaks. Figure 5 gives a typical time sequence recorded for fraction

TABLE 2
Fatty Acid Profiles of Fractions Obtained by Acetone Fractionation

		Fraction[a]											
Fatty acid	Milk fat	S25	S20	S15	S10	S5	S2	S0	S–5	S–13	S–20	S–25	L–25
$C_{4:0}$	3.68	2.67	1.19	1.21	1.68	2.27	3.41	3.92	3.97	3.80	4.41	4.16	5.99
$C_{6:0}$	2.45	1.65	0.76	0.83	1.07	1.59	2.27	2.46	2.36	2.31	2.73	3.00	3.55
$C_{8:0}$	1.35	1.04	0.49	0.66	0.72	1.03	1.27	1.26	1.24	1.41	1.65	2.03	2.13
$C_{10:0}$	3.19	2.54	1.40	2.53	2.20	2.77	2.73	2.50	2.78	3.36	4.12	4.96	4.15
$C_{12:0}$	4.40	3.90	2.87	5.22	4.29	3.61	2.86	2.57	3.74	4.92	6.38	6.42	4.87
$C_{14:0}$	11.91	12.57	13.20	15.37	14.19	9.97	9.72	10.45	13.86	14.55	14.70	11.65	9.03
$C_{16:0}$	32.97	37.99	44.83	39.76	41.04	41.28	46.19	45.82	37.65	28.93	27.93	26.39	17.85
$C_{18:0}$	10.09	14.38	19.31	13.15	13.86	17.28	12.34	12.16	10.08	8.20	8.39	8.36	4.47
$C_{18:1}$	19.34	14.41	9.62	13.41	13.02	13.15	12.42	11.65	15.43	21.76	26.78	29.29	42.19
$C_{18:2}$	2.17	1.26	1.07	1.21	1.20	1.15	1.03	1.13	1.47	1.89	3.85	3.74	5.76

[a]See Table 1 for abbreviations and explanation.

TABLE 3
Acyl Chain-Length Profile for Fractions Obtained by Acetone Fractionation

TG number[b]	Fraction[a]												
	Milk fat	S25	S20	S15	S10	S5	S2	S0	S–5	S–13	S–20	S–25	L–25
26	0.2	0.1	0.0	0.0	0.1	0.0	0.0	0.0	0.0	0.1	0.5	0.6	1.4
28	0.6	0.4	0.1	0.1	0.2	0.1	0.1	0.1	0.2	0.4	1.2	1.1	2.9
30	1.2	0.8	0.3	0.3	0.5	0.2	0.2	0.2	0.4	0.8	2.1	2.4	5.1
32	2.8	1.8	0.7	0.7	1.0	0.4	0.6	0.6	1.1	2.5	5.8	7.9	8.1
34	6.5	4.1	1.7	1.8	2.6	1.6	2.9	4.1	6.6	9.7	15.8	15.5	9.3
36	12.4	7.9	3.5	3.8	5.1	7.2	14.7	17.9	17.9	14.2	17.4	13.7	12.8
38	14.1	9.0	4.0	4.7	6.0	11.4	15.9	17.2	15.4	13.0	15.2	13.2	20.2
40	10.8	7.2	3.5	5.2	5.4	9.5	10.8	10.9	10.9	10.3	10.0	10.2	15.1
42	8.0	6.6	4.2	9.4	7.0	10.9	10.7	9.4	7.7	6.6	6.3	8.5	7.7
44	7.5	8.1	7.7	15.3	11.6	11.8	7.9	6.2	5.6	6.5	6.9	8.8	4.5
46	7.8	11.0	15.2	16.8	16.5	9.0	5.9	5.1	6.1	7.7	6.8	5.9	2.6
48	8.8	14.0	21.7	14.4	16.4	8.4	7.6	7.9	9.9	9.1	5.2	3.4	2.4
50	9.6	15.6	22.2	15.0	15.7	14.7	13.9	12.3	9.5	7.5	0.8	0.4	3.0
52	7.3	10.6	12.2	9.9	9.5	12.1	7.5	6.9	6.8	8.4	4.5	5.4	2.9
54	2.2	2.8	2.8	2.6	2.5	2.6	1.5	1.4	2.0	3.2	1.5	3.1	1.9

[a]See Table 1 for abbreviations and explanation.
[b]TG, triglyceride; TG number, number of carbon atoms present in the fatty acid chains of the TG molecule.

S30 at a temperature of 23°C, showing a pattern typical for α-crystals at the start of the isothermal period, and the transformation into a pattern typical for β′-crystals starting at 7 min and ending at 12 min. The results of the XRD measurements on fraction S30 are listed in Table 7. Apparently, the first peak in the DSC curve corresponds to a maximum of the crystallization rate during the formation of α-crystals, while the second peak is due to a maximum of the crystallization rate during the formation of β′-crystals. At the lower temperatures, a part of the α-crystals remained present after the formation of β′-crystals had ended.

Similar behavior was also observed for the other fractions and also for whole milk fat (3). XRD measurements confirmed that for all fractions, the first and second exothermic maxima correspond to the formation of α- and β′-crystals. In Figure 6, the measured times of the second exothermic maximum are plotted as a function of temperature for isothermal crystallization of the various fractions. In general, the induction time for the formation of β′-crystals from milk fat fractions is seen to increase at higher temperatures. Moreover, at a given temperature, the induction time is larger for fractions with a lower clear point of the β′-form. Deviations from this monotonic increase of the induction time with temperature are seen to occur. These are most obvious for the HMT fractions S30 and S24. The stable crystal form was found to be the β′-form for all fractions. Even fraction L11 was crystallized into the β′-form after storage for 2 wk at 4°C.

DSC heating curves recorded after isothermal crystallization of fractions obtained by dry fractionation. The phase transitions occurring during isothermal crystallization were investigated further by recording the DSC heating curves after varying periods of isothermal crystallization. As a typical example, Figure 7 shows the resulting curves for dry fraction S30 after isothermal crystallization at 23°C. During the first 5 min, the growth of a peak is observed, which disappears upon heating in the temperature range of 25–32°C. This peak corresponds to the first crystallization peak in Figure 4 and is due to the formation of α-crystals. After 5 min, a second peak starts to form, which disappears upon heating in the temperature range of 30–42°C. This peak corresponds to the second crystallization peak in Figure 4, which is due to the formation of β′-crystals. After 6 to 10 min, the α-crystals disappear, while the quantity of fat crystallized in the β′-form increases. The maximum increase in the quantity of fat crystallized in the β′-form occurs between 10 and 15 min. After 30 min, the final shape of the β′-melting peak is reached, which means that the crystallization process had ended.

Crystallization of dry fraction S30 was also investigated at −10°C. XRD measurements showed the presence of α-crystals during the whole measuring time of 30 min and the slow formation of a small amount of β′-crystals during this period (data not shown). DSC heating curves were also recorded for dry fraction S30 after a series of isothermal crystallization times at

TABLE 4
Relative Amounts and Clear Points of the Fractions Obtained by Dry Fractionation[a]

Fraction[b]	Relative amount (weight %)	Clear point (°C)
Milk fat	100	36.4
S24	63	40.0
S30	24	41.4
L30	39	33.1
L24	37	24.0
S19	22	27.5
L19	15	—[c]
S11	7	17.9
L11	7	10.3

[a]Due to the procedure of preparation the combinations the relative amounts sum up according to S24 + L24 = 100%; S24 = S30 + L30; L24 = S19 + L19; L19 = S11 + L11.
[b]S, solid; L, liquid numbers following the type of fraction (S or L) correspond to the temperature at which the filtrate fractionated (11 to −30°C).
[c]Not determined.

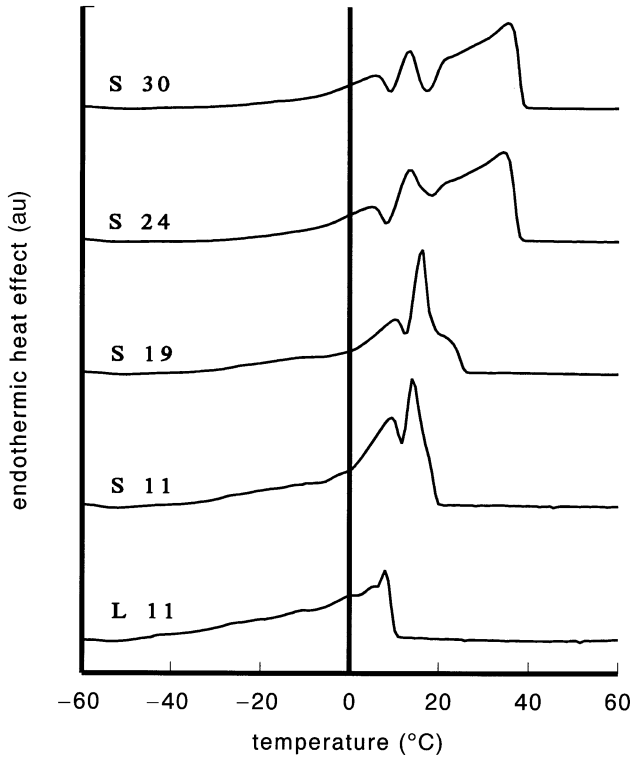

FIG. 3. DSC heating curves of the dry fractions. See Figure 2 for abbreviations.

−10°C (Fig. 9). The curve recorded after 1 min starts with an endothermic heat effect, which according to the XRD measurements must be due to the melting of α-crystals. In the temperature region of 8–20°C, an exothermic heat effect is observed, followed by an endothermic shoulder between 20 and 39°C that strongly resembles the melting range of β′-crystals of HMT. Apparently, the exothermic effect between 8 and 20°C is due to the formation of these β′-crystals. DSC heating curves recorded after longer isothermal crystallization times show the gradual disappearance of the exothermic effect between 8 and 20°C, which is simultaneous with the gradual growth of a sharp endothermic peak in the same region. Most likely, this sharp endothermic peak is due to the melting of β′-crystals of MMT. Apparently, during isothermal storage at −10°C, β′-crystals of HMT and MMT grow simultaneously.

DISCUSSION

The experimental results show that milk fat fractions can be divided into three main groups: HMT, MMT, and LMT. LMT is enriched in the short-chain fatty acids (Table 2). Note that the short-chain fatty acids $C_{4:0}$ and $C_{6:0}$ have a joint weight fraction of almost 9% of the total fatty acids in fraction L–25 (corresponding to 20% on a molar basis). Taking into account that $C_{4:0}$ and $C_{6:0}$ are almost exclusively found at the *sn*-3 position (22), this proves that fraction L–25 mainly consists of triglycerides with a short-chain fatty acid in the *sn*-3 position. This explains the observed low position of the maximum in the acyl-carbon number profile (Table 3). Furthermore, almost half of the fatty acids in L–25 are unsaturated. The combination of short-chain fatty acids and unsaturated fatty acids leads to the observed low melting point of this fraction. The other LMT fractions have a composition similar to L–25. However, they contain somewhat more $C_{16:0}$ and somewhat less $C_{18:1}$. HMT contains hardly any short-chain fatty acids, which leads to the observed high values of the acyl-carbon numbers (Table 3). HMT is also reduced in unsaturated fatty acids, which explains the high melting point of this group of triglycerides. The important finding that HMT and MMT crystallize separately supports the view that these really may be distinguished as two different groups of triglycerides. Compared to HMT, MMT contains relatively much $C_{16:0}$ and $C_{4:0}$. MMT seems to form a group between HMT and LMT, which probably contains molecules that either possess a $C_{4:0}$ or a combination of two unsaturated fatty acids or other combinations that will result in a melting point somewhat lower than that of the HMT group. This also explains the occurrence of two maxima in the acyl-carbon number profile (Table 3).

All fractions were seen to crystallize in the α- or β′-phase, of which the former was seen to be metastable. At high cooling rates, crystallization in the metastable γ-phase was also observed (not shown), similar to the occurrence of this phase in milk fat (3). The β-crystal form was not detected in any of the samples obtained by dry fractionation. In the literature of

TABLE 5
Fatty Acid Profiles of the Main Groups of Fatty Acids for the Various Fractions Obtained by Dry Fractionation[a]

Fatty acid	Milk fat	S24	S30	L30	L24	S19	L19	S11	L11
$C_{4:0}$	3.83	3.37	3.21	4.32	4.19	3.32	4.49	4.11	4.52
$C_{6:0}$	2.37	2.10	1.98	2.32	2.61	2.10	2.74	2.50	2.77
$C_{8:0}$	1.39	1.27	1.20	1.39	1.49	1.29	1.58	1.50	1.75
$C_{10:0}$	3.13	2.97	2.86	3.16	3.18	3.17	3.37	3.35	3.81
$C_{12:0}$	4.43	4.44	4.37	4.46	4.18	4.72	4.44	4.61	5.06
$C_{14:0}$	11.99	12.35	12.44	11.93	11.23	12.65	11.38	12.52	11.40
$C_{16:0}$	32.37	33.94	34.80	31.85	32.88	32.95	29.72	29.3	22.79
$C_{18:0}$	9.63	10.58	10.99	9.40	9.19	10.03	8.33	9.03	6.37
$C_{18:1}$	21.05	19.47	18.80	21.32	21.28	19.86	23.50	22.09	28.55
$C_{18:2}$	1.94	1.85	1.81	1.94	1.91	1.87	2.09	2.12	2.61

[a]Standard deviation 0.1%.
[b]See Table 2 for abbreviations and explanation.

TABLE 6
Acyl Chain Length Distribution for the Various Fractions Obtained by Dry Fractionation[a]

	Fraction[b]								
TG number[c]	Milk fat	S24	S30	L30	L24	S19	L19	S11	L11
26	0.2	0.2	0.2	0.2	0.2	0.2	0.2	0.2	0.3
28	0.6	0.5	0.5	0.6	0.6	0.5	0.8	0.6	1.0
30	1.2	1.0	1.0	1.2	1.3	1.0	1.6	1.3	2.1
32	2.8	2.4	2.4	2.8	2.9	2.3	3.4	3.1	4.4
34	6.5	5.7	5.7	6.4	7.0	5.5	7.7	7.7	8.0
36	12.4	10.7	11.0	12.1	14.1	10.5	13.9	12.9	11.4
38	14.1	12.3	12.7	13.9	15.6	12.3	15.7	14.5	14.8
40	10.8	9.9	10.1	10.7	11.3	10.0	12.1	11.4	12.6
42	8.0	8.0	8.5	8.1	8.1	8.8	7.7	7.7	7.5
44	7.5	8.2	9.3	7.6	6.8	8.9	6.3	6.5	6.0
46	7.8	9.2	10.8	7.7	6.4	9.0	6.0	6.4	6.0
48	8.8	10.2	12.0	8.6	7.2	9.7	6.8	7.7	6.6
50	9.6	11.1	12.8	9.8	8.9	10.7	8.0	8.9	7.1
52	7.3	7.9	8.4	7.6	7.1	7.9	7.0	8.1	8.3
54	2.2	2.4	2.4	2.4	2.2	2.3	2.4	3.0	3.8

[a]Acyl chain length distribution is expressed as a percentage of the sum of weights of fatty acids. Standard deviation 5% of the value.
[b]See Table 4 for abbreviations and explanation.
[c]See Table 3 for abbreviation and explanation.

milk fat crystallization, larger amounts of the β-modification were only observed in a HMF fraction obtained by acetone fractionation (4,23,24). However, total crystallization in the β-form proved to be difficult (4). Timms (16) stated that the acetone HMF fractions of milk fat can only crystallize in the β-form in the presence of a LMF fraction of milk fat obtained by acetone fractionation.

An important physical aspect of the fractions lies in the rate of crystallization into the β′-form. The general behavior observed in Figure 6 is that the lower the melting point of the fat fraction, the longer the induction time for crystallization. This result is in agreement with the results of Sato and Kuroda (25) on the crystallization of trilaurin and in general for the crystallization of pure liquids. Theoretically, the induction time for crystallization can be explained qualitatively by nucleation theory. For pure liquids at low supercooling, the lag time L needed to form crystal embryos of sufficiently large size to nucleate crystal growth is described by an equation of the form (26)

$$L = A \cdot \exp\left(\frac{B}{kT} \cdot \frac{1}{\Delta\Psi^2}\right) \quad [1]$$

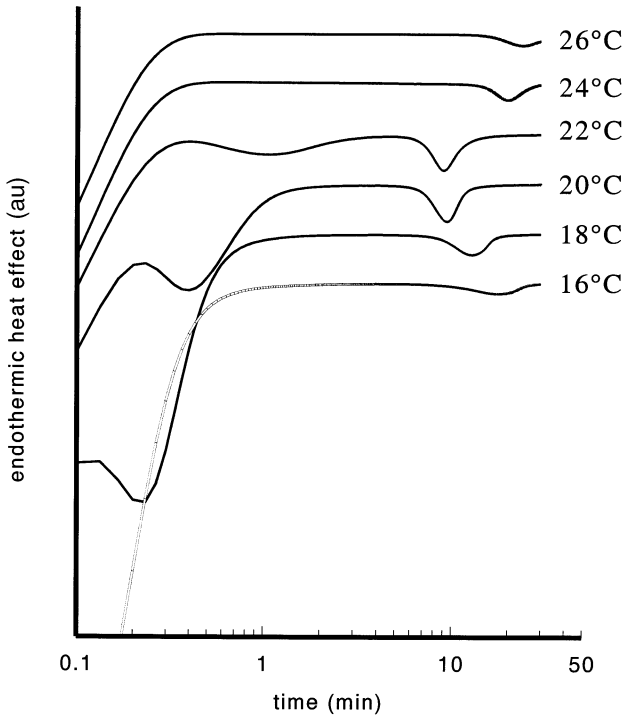

FIG. 4. Isothermal DSC curves recorded for dry fraction S30 at various temperatures. S30, solid fraction produced when filtered at 30°C; see Figure 2 for other abbreviations.

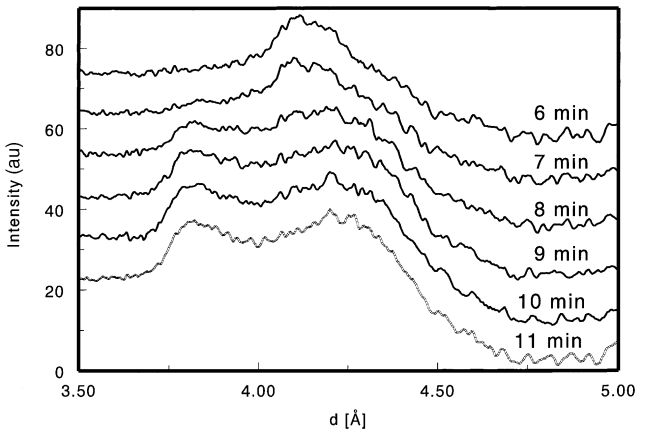

FIG. 5. Sequence of X-ray diffraction (XRD) curves recorded for dry fraction S30 at 23°C. No changes were observed during the first 6 min. See Figure 4 for abbreviation.

TABLE 7
Isothermal Crystallization of Milk Fat Fraction S30[a]

T (°C)	t_s (min)	t_m (min)	t_e (min)	Phase at $t = 0$	Final phase
–10	8	15	30	α	α + β′
7	6	14	28	α	α + β′
14	6	14	21	α	α + β′
20	7	11	14	α	α + β′
23	7	8	12	(α)[b]	(α) + β′

[a]S30, solid fraction produced when filtered at 30°C; t_s = start of the transformation, t_m = maximum rate of transformation, t_e = end of transformation.
[b]Parentheses indicate that the polymorphic form was observed only in minor amounts.

where k is Boltzmann's constant, T is absolute temperature, and A and B are constants, depending on model parameters such as the surface tension of the embryos and the molecular volume of the triglyceride molecules. The parameter $\Delta\Psi$ is the decrease in free energy for the incorporation of a triglyceride molecule in the crystal embryo, which can be estimated from

$$\Delta\Psi = \theta\Delta S_f \qquad [2]$$

where ΔS_f is the molecular entropy of fusion at the melting temperature T_m; $\Delta H_f = T_m \cdot \Delta S_f$; and θ is the supercooling $T - T_m$. These equations predict that the time lag for nucleation increases strongly when the melting point is reached, and that at the same temperature, longer induction times for crystallization will be found for fractions with lower melting point. This behavior can be observed in Figure 6.

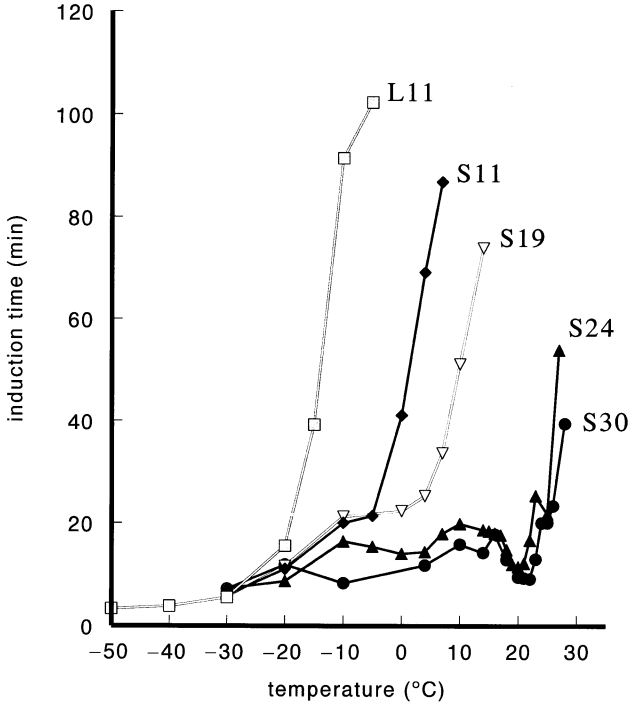

FIG. 6. Induction times for isothermal crystallization of β′-crystals of fractions obtained by dry fractionation.

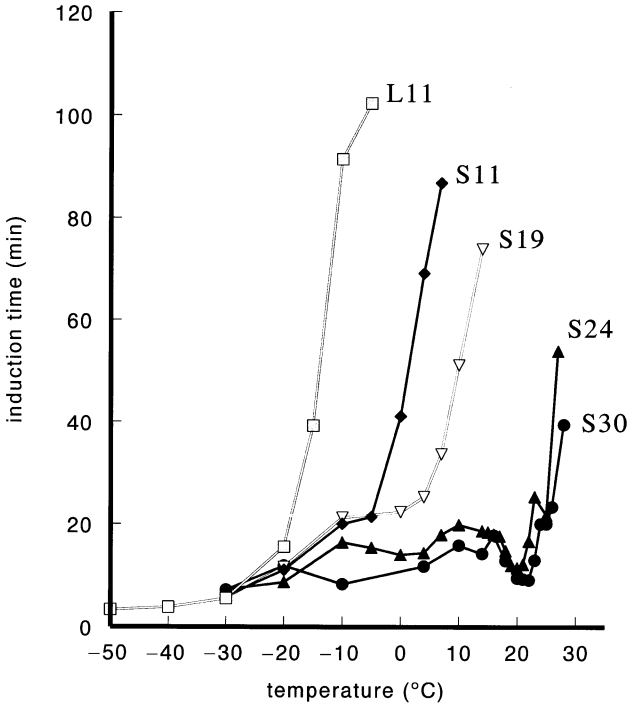

FIG. 7. DSC heating curves recorded after various periods (min) of isothermal crystallization at a temperature of 23°C of dry fraction S30. See Figures 2 and 4 for abbreviations.

The crystallization properties of the lower-melting milk fat fractions can be explained from their molecular structure. The highly asymmetric molecular structure of these fractions leads to a much less favorable incorporation of the molecules into the β′-crystal lattice. This results in a lower melting point and a reduced driving force for nucleation and crystal growth. This also explains why the separation of lower-melting fractions is much more difficult than the separation of higher- melting fractions. For good separation (agglomerated) crystals in the β′-form are favorable (12,27,28). The formation of these will take much longer for the lower-melting fractions. Also the slow "setting" of milk fat after crystallization may be a result of the very slow β′-crystallization of MMT and especially LMT.

The separate crystallization of HMT and MMT in the high-melting dry fractions observed in Figure 8 explains the deviating relationship between the induction time for β′-crystallization vs. the temperature observed in Figure 6. At higher temperatures (>20°C), one observes the induction time for the crystallization of β′-crystals of HMT, whereas at lower temperatures (<16°C) the induction time of a mixture of β′-crystals of MMT and HMT is measured. In a small transition region, the effective induction time of mixed β′-crystals decreases with temperature.

The differentiation into three groups, HMT, MMT, and LMT, found by us differs from the differentiation into HMF, MMF, and LMF frequently used the literature. The latter distinction is based on an *a priori* choice of the fractionation temperature in their solvent fractionation. HMF corresponds to the higher melting fractions of HMT, whereas MMF corresponds to the lower melting fractions of our HMT. LMF corresponds to a

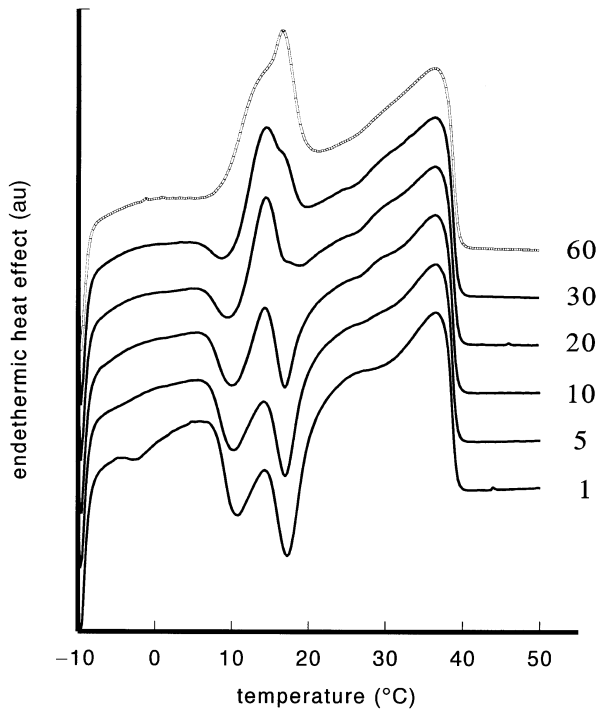

FIG. 8. Material and conditions were the same as Figure 7, but at a temperature of –10°C.

combination of our MMT and LMT. The experimental result of Marangoni and Lenki (17) that showed MMF and HMF cocrystallize into mixed crystals forming solid solutions, and that the combinations LMF–HMF and LMF–MMF form partial solid solutions, therefore corresponds well with our findings.

ACKNOWLEDGMENTS

The authors thank Franklin D. Zoet for carrying out the fractionations and most of the DSC measurements and Zeno E.H. Otten and Rob Dekker for carrying out part of the DSC and the analytical measurements, respectively. Richard Kranenburg and Jaap van Asselt are thanked for running the dry-fractionation setup. Kees Van Malssen is acknowledged for useful advice and allowing us to use his XRD equipment. This project was supported by The Netherlands Ministry of Agriculture, Nature Management and Fisheries.

REFERENCES

1. Larsson, K., Alternation of Melting Points in Homologous Series of Long-Chain Compounds, *J. Am. Oil Chem. Soc. 43*:559–562 (1966).
2. Timms, R.E., Phase Behaviour of Fats and Their Mixtures, *Prog. Lipid Res. 23*:1–38 (1984).
3. ten Grotenhuis, E., G.A. van Aken, K.F. van Malssen, and H. Schenk, Polymorphism of Milk Fat Studied by Differential Scanning Calorimetry and Real-Time X-ray Powder Diffraction, *J. Am. Oil Chem. Soc. 76*:1031–1039 (1999).
4. Belousov, A.P., and V.M. Vergelesov, Polymorphism in Butter Fat, *Int. Dairy Congr. [Proc.] 16th* B122 (1962).
5. Van Malssen, K.F., Real-Time X-ray Diffraction Applied to Cocoa Butter and Graphite Intercalates, Ph.D. Thesis, University of Amsterdam, The Netherlands (1994).
6. Wesdorp, L.H. Liquid-Multiple Solid Phase Equilibria in Fats—Theory and Experiments, Ph.D. Thesis, Delft University, The Netherlands (1990).
7. Antilla, V., Fractionated Milk Fat, *Int. Dairy Cong*., *[Proc] 23rd 3*:1980–1986 (1991).
8. Antilla, V., The Fractionation of Milk Fat, *Milk Ind. 81*:17–20 (1979).
9. Kaylegian, K.E., and R.C. Lindsay, *Handbook of Milkfat Fractionation Technology and Applications*, AOCS Press, Champaign, 1995.
10. Amer, M.A., D.B. Kupranyez, and B.E. Baker, Physical and Chemical Characteristics of Butter Fat Fractions Obtained by Crystallization from Molten Fat, *J. Am. Oil Chem. Soc. 62*:1551–1557 (1985).
11. Dimick, P.S., S. Yella Reddy, and G.R. Ziegler, Chemical and Thermal Characteristics of Milk-Fat Fractions Isolated by a Melt Crystallization, *Ibid. 73*:1647–1652 (1996).
12. Deffense, E., Multi-Step Butteroil Fractionation and Spreadable Butter, *Fat Sci. Technol. 13*:502–507 (1987).
13. Deffense, E., Milk Fat Fractionation Today: A Review, *J. Am. Oil Chem. Soc. 70*:1193–1201 (1993).
14. Kumar, P., and P.N. Thakar, Fractionation of Milk Fat—Processes Used and Properties of Fractions—A Review, *Ind. J. Dairy Sci. 48*:1–11 (1995).
15. Rajah, K.K., Fat Products Using Fractionation and Hydrogenation, in *Fats in Food Products*, edited by D.P.J. Moran and K.K. Rajah, Blackie Academic & Professional, London, 1994, pp. 277–317.
16. Timms, R.E., The Phase Behaviour and Polymorphism of Milk Fat, Milk Fat Fractions, and Fully Hardened Milk Fat, *Aust. J. Dairy Technol. 35*:47–53 (1980).
17. Marangoni, A.G., and R.W. Lencki, Ternary Phase Behavior of Milk Fat Fractions, *J. Agric. Food Chem. 46*:3879–3884 (1998).
18. Timms, R.E., The Phase Behaviour of Mixtures of Cocoa Butter and Milk Fat, *Lebensm. Wiss. Technol. 13*:61–65 (1980).
19. Badings, H.T., and C. de Jong, Glass Capillary Gas Chromatography of Fatty Acid Methyl Esters. A Study of Conditions for the Quantitative Analysis of Short- and Long-Chain Fatty Acids in Lipids, *J. Chromatogr. 279*:493–506 (1983).
20. Van Malssen, K.F., R. Peschar, and H. Schenk, Geometrical Aspects of Real-Time Powder Diffraction Using a Normal Generator and a Linear Diode Array Detector, *J. Appl. Cryst. 27*:302–315 (1994).
21. Lohman, M.H., and R.W. Hartel, Effect of Milk Fat Fractions on Fat Bloom in Dark Chocolate, *J. Am. Oil Chem. Soc. 71*:267–276 (1994).
22. Kuksis, A., L. Marai, and J.J. Myher, Triglyceride Structure of Milk Fats, *Ibid. 50*:193–201 (1973).
23. Schaap, J.E., H.T. Badings, D.G. Schmidt, and E. Frede, Differences in Butterfat Crystals, Crystallized from Acetone and from the Melt, *Neth. Milk Dairy J. 29*:242–252 (1975).
24. Woodrow, I.L., and J.M. deMan, Polymorphism in Milk Fat Shown by X-Ray Diffraction and Infrared Spectroscopy, *J. Dairy Sci. 51*:996–1000 (1968).
25. Sato, K., and T. Kuroda, Kinetics of Melt Crystallization and Transformation of Tripalmitin Polymorphs, *J. Am. Oil Chem. Soc. 64*:124–127 (1987).
26. Buckle, E.R., Studies on the Freezing of Pure Liquids, II. The Kinetics of Homogeneous Nucleation in Supercooled Liquids, *Proc. R. Soc. Ser. A 261*:189–196 (1961).
27. Voss, E., U. Beyerlein, and E. Schmanke, Probleme der Technischen Fraktionierung von Butterfett mit Hilfe des Fettkörnchen-Filtrationsverfahrens, *Milchwissenschaft 26*:605–613 (1971).
28. Schaap, J., and G.A.M. Rutten, Effect of Technological Factors on the Crystallization of Bulk Milk Fat, *Neth. Milk Dairy J. 30*:197–206 (1976).

[Received November 23, 1998; accepted July 20, 1999]